# Robust Performance Verification of Adaptive Robust Controller for Hard Disk Drives

Hamid D. Taghirad, *Member, IEEE*, and Ehsan Jamei

***Abstract*—An adaptive robust controller (ARC) has been recently developed for read/write head embedded control systems of hard disk drives (HDDs). This structure is applicable to both track seeking and track following modes, and it makes the mode switching control algorithms found in conventional HDD servosystems unnecessary. An Improved Desired Compensation ARC (IDCARC) scheme is proposed in this paper, in which the traditional ARC is powered by a dynamic adaptive term. In this approach the adaptation regressor is calculated using reference trajectory information. Moreover, a robust analysis of this method is developed, in which a controller designed based on a simple model of the system is verified in a closed loop performance of a more comprehensive model of the system. The simulation result verifies the significant improvement of the performance of IDCARC compared to that of ARC and its robustness for this model. It is observed that in the presence of large disturbances the proposed method preserves the stability and a suitable performance while the ARC fails even in stability.**

***Index Terms*—Adaptive robust control, dynamic adaptation, hard disk drive (HDD), nonlinear robust control, robustness verification.**

## I. Introduction

HARD DISK servosystems play a vital role in the demand for increasingly high density and high performance hard disk drives (HDDs). The servosystem must achieve precise positioning of the read/write head on a desired track (track following) and fast transition from one track to another target track (track seeking). The seeking time should be minimized for faster data transmission rates. Because of the different control objectives in seeking and following modes, many drives use mode switching control (MSC) to accomplish both tasks. In MSC, nonlinear controller routines such as proximate time optimal servo (PTOS) are popular choices for track seeking [1]. For track following, adaptive control [2], [3], repetitive control, and many other approaches have been developed [4]–[10]. The switching of control mode from track seeking to track following should be so smooth that the residual vibration of the suspension is minimal [4]. There have been several attempts to develop unifying control algorithms that work for both track seeking and following. Such control algorithms utilize the two degrees-of-freedom control structure [4]–[6], composite nonlinear feedback control [7], gradient-based track following [8], or other robust approaches for control [9], [10]. Yi and Tomizuka [3] proposed a two degrees-of-freedom adaptive robust controller (ARC) for the HDD in which track seeking is accomplished by use of a feedforward controller based on offline identification. Xu and Yao [11] proposed the Desired Compensation ARC (DCARC) for linear motors in which the adaptation regressor is calculated using trajectory information based on the work of Sadegh and Horowitz [12]. We have proposed earlier an Improved DCARC (IDCARC), which includes a dynamic adaptation mechanism to achieve hard disk performance necessities, such as fast disturbance attenuation and accuracy [13].

In this paper, this unifying controller structure is described based on IDCARC, and its closed loop performance is verified in the presence of high frequency resonant modes in the model. IDCARC combines DCARC advantages [11], in addition to faster disturbance attenuation, which is obtained through a dynamic adaptation routine included in the structure [6]. The algorithm can be easily implemented as a unified embedded controller on both seeking and following modes. The reference trajectory is generated based on structural vibration minimized acceleration (SMART), in which the residual vibration of the suspension is minimal [4]. Hence, the reference trajectory and its second-order derivation, which is necessary in this ARC method, are generated online, and the differentiation from the reference input becomes unnecessary. Moreover, the reference input signals based on SMART strategy will prevent saturation [4]. The proposed new ARC controller has important advantages such as separating robust control design from the parameter adaptation process [12], reducing the effect of measurement noise on the tracking, making the adaptation process faster, and reducing the need for feedforward control in seeking time. The controller also considers the delay in seeking time, the model uncertainties, and the effect of pivot friction. To fulfill the high performance requirements, the model considered in the controller performance verification includes most significant nonlinear effects, namely the friction and the high frequency resonant modes. Hence, the simulation results applied in this model are promising for actual application.

In the next section, the plant modeling and problem formulation is introduced. In Section III, the adaptive robust algorithm (DCARC) and the proposed IDCARC are introduced and their robust stability is analyzed. Finally, the comparative studies are elaborated in Section IV.

Manuscript received April 30, 2005; revised September 17, 2007.

H. D. Taghirad is with the Advanced Robotics and Automated Systems (ARAS) Research Group, Department of Electrical Engineering, and the Office of International and Scientific Cooperation, K. N. Toosi University of Technology, Tehran 16315-1355, Iran (e-mail: Taghirad@kntu.ac.ir).

E. Jamei is with the Advanced Robotics and Automated Systems (ARAS) Research Group, Department of Electrical Engineering, K. N. Toosi University of Technology, Tehran 16315-1355, Iran.

Color versions of one or more of the figures in this paper are available online at http://ieeexplore.ieee.org.

Digital Object Identifier 10.1109/TIE.2007.896502

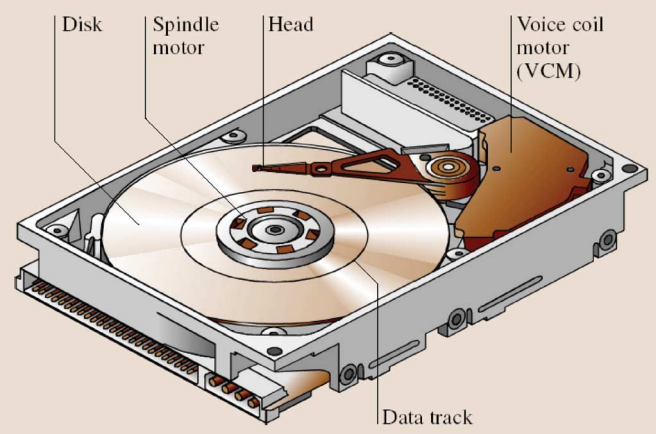


Fig. 1. HDD components.

## II. Problem Formulation and Dynamical Models

A comprehensive mathematical model of the hard disk servodrive system is given as follows [1], [9]:

$$\begin{cases} \dot{x}_1 = x_2 \\ J\dot{x}_2 = u - Bx_2 - A_{\rm f}\mathrm{Sign}(\dot{y}) - F_{\rm hys} + F_{\rm hi} + F_{\rm d} \end{cases} \qquad y = x_1 \quad (1)$$

in which, $x = [x_1, x_2]^{\rm T}$ represent the state vector of the angular position and velocity, $y$ is the position, $J$ is the moment of inertia, $u$ is the control input, $B$ and $A_{\rm f}$ are coefficient of viscous and Coulomb friction, respectively, $F_{\rm hys}$ and $F_{\rm hi}$ represent the effect of hysteresis loop and high frequency uncertainties, respectively, and, $F_{\rm d}$ is the external disturbance. Let $y_{\rm r}$ be the reference motion trajectory. The control objective is to synthesize a control input $u$ such that the output $y$ tracks $y_{\rm r}(t)$ as close as possible, despite various model uncertainties.

Fig. 1 shows the different components of the HDD, and the parameters used in the simulations are given in Table I. A simpler version of the model, in which the hysteresis, high frequency resonance, and the external disturbances are considered as uncertain disturbances, is assumed to be the basis of the ARC design. However, for robustness verification of the closed loop performance, a more comprehensive model including high frequency resonance modes [1] is used. The transfer function of the more comprehensive system is derived from identification experiments, and its frequency response is illustrated in Fig. 2. The model is identified using least-squares estimation on the frequency response. The identified transfer function is a tenth-order nonminimum phase system, with two real poles, one of them right at the origin and another one close to the origin, which resembles the dynamical behavior reported in [9]. The identified poles are: $10^4 \times (0, -0.0012, -0.0283 \pm 5.6548i, -0.1257 \pm 2.510i, \ -0.0069 \pm 1.3823i, -0.0022 \pm 0.0439i)$. Moreover, the zeros are located at: $10^5 \times (-6.8070, 0.0017 \pm 0.4360i, -0.0008 \pm 0.1394i, -0.0002 \pm 0.0044i)$.

In Fig. 2, the frequency response of the simple model (dash dot) is compared to that of a more comprehensive model (solid). The input to the system is the VCM current measured in (milliampere) and the output of the system is the head position in (millimeter). As seen in Fig. 2, the more comprehensive model contains a resonance frequency of about 2200 Hz. The consistency of the simplified model to the more comprehensive model is clearly illustrated by the perfect fit at low frequencies. The controller design goal is to obtain desired tracking performance and to avoid exciting high frequency modes especially during the following mode.

TABLE I
Parameter of HDD Components

| Description | Symbols | Quantity |
|---|---|---|
| Spindle speed | $\omega$ | 3623 *rpm* |
| Track pitch | $L_{track}$ | $1\,\mu m$ |
| Coil resistance and Current sensing resistance | $R$ | $8.516\,\Omega$ |
| Viscous Friction | $B$ | $2.54\ \ N\cdot\sec/m$ |
| Torque constant | $K_T$ | $20\ \ N/A$ |
| Moment of inertia | $I_b$ | $12.5\times10^{-6} kg\cdot m^2$ |

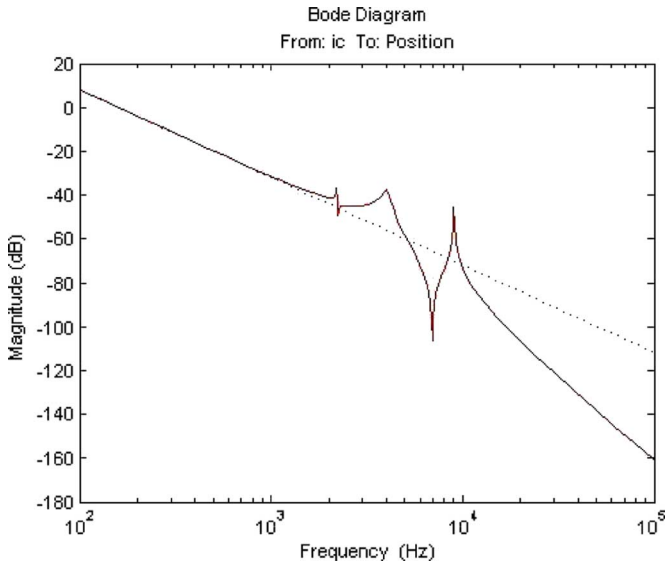


Fig. 2. Bode diagram of HDD ideal model (dashed) and more complete model (solid).

## III. Adaptive Robust Control

To design the ARC, identification of a simple model for the system is sufficient. The state space representation of this model can be linearly parameterized as

$$\dot{x}_1 = x_2 \quad (2)$$

$$\theta_1\dot{x}_2 = u - \theta_2 x_2 - \theta_3 \mathrm{Sign}(x_2) + \theta_4 + \tilde{d}. \quad (3)$$

In which $\theta_4 = d_n$ is the nominal value of the lumped disturbance $d$. It is assumed that all the effects of hysteresis and high frequency resonance is absorbed into the term $d$. To describe the controller structure, consider the following assumptions.

*Assumptions:* The following bounds and structures for uncertainties and disturbances are assumed:

$$\theta \in \Omega_\theta \equiv \{\theta : \theta_{\min} < \theta < \theta_{\max}\} \quad (4)$$

$$\tilde{d} \in \Omega_{\rm d} \equiv \{\tilde{d} : |\tilde{d}| < \delta_{\rm d}\}. \quad (5)$$

In which, $\theta_{\min} = [\theta_{1\min}, \ldots, \theta_{4\min}]^{\mathrm{T}}$, $\theta_{\max} = [\theta_{1\max}, \ldots, \theta_{4\max}]^{\mathrm{T}}$ and $\delta_{\mathrm{d}}$ are assumed to be known. Let $\hat{\theta}$ denote the estimate of $\theta$ and $\tilde{\theta}$ the estimation error (i.e., $\tilde{\theta} = \hat{\theta} - \theta$). In view of (4) the following adaptation law with discontinuous projection modification can be used:

$$\dot{\hat{\theta}} = \mathrm{Proj}(\Gamma\tau) \tag{6}$$

where $\Gamma > 0$ is a diagonal matrix, $\tau$ is adaptation function to be synthesized later. The projection mapping is defined as

$$\mathrm{Proj}_{\hat{\theta}}(g) = \left[\mathrm{Proj}_{\hat{\theta}_1}, (g_1), \ldots, \mathrm{Proj}_{\hat{\theta}p}(g_p)\right]^{\mathrm{T}}$$
$$\mathrm{Proj}_{\hat{\theta}_i}(g_i) = \begin{cases} 0, & (\text{if } \hat{\theta}_i = \theta_{i\max} \text{ and } g_i > 0) \\ & \quad \text{or (if } \hat{\theta}_i = \theta_{i\min} \text{ and } g_i < 0) \\ g_i & \text{Otherwise.} \end{cases} \tag{7}$$

It can be shown that for any adaptation function $\tau$ the projection mapping used in (7) guarantees [15]

$$\begin{aligned} &\text{P1} \quad \hat{\theta} \in \Omega_\theta \equiv \{\hat{\theta} : \theta_{\min} \le \hat{\theta} \le \theta_{\max}\} \\ &\text{P2} \quad \tilde{\theta}^{\mathrm{T}}(\Gamma^{-1}\mathrm{Proj}(\Gamma\tau) - \tau) \le 0 \qquad \forall\tau. \end{aligned} \tag{8}$$

### A. ARC Controller Design

Define a switching-function quantity as $p = \dot{e} + k_1 e = x_2 - x_{2\mathrm{eq}}$, where $x_{2\mathrm{eq}} \equiv \dot{y}_{\mathrm{d}} - k_1 e$ and $e = y - y_{\mathrm{d}}(t)$ is the output tracking error, $y_{\mathrm{d}}(t)$ is the desired trajectory to be tracked by $y$, and $k_1$ is any positive feedback gain. With respect to (3) one can obtain

$$\begin{aligned} J\dot{p} &= u - \theta_1\dot{x}_{2\mathrm{eq}} - \theta_2 x_2 - \theta_3 \mathrm{Sign}(x_2) + \theta_4 + \tilde{d} \\ &= u + \varphi^{\mathrm{T}}\theta + \tilde{d}. \end{aligned} \tag{9}$$

If $p$ is small or converges to zero exponentially, then the output tracking error $e$ will be small or converge to zero exponentially. This is because $G_p(s) = e(s)/p(s) = 1/(s + k_1)$ is a stable transfer function. Hence, the rest of the design is to make $p$ as small as possible. Where $\varphi^{\mathrm{T}} = [-\dot{x}_{2\mathrm{eq}}, -x_2, -\mathrm{Sign}(x_2), 1]$ and $\dot{x}_{2\mathrm{eq}} = \ddot{y}_{\mathrm{d}} - k_1\dot{e}$.

The control law consists of two parts

$$\begin{aligned} u &= u_{\mathrm{a}} + u_{\mathrm{s}}, \qquad u_{\mathrm{a}} = -\varphi^{\mathrm{T}}\hat{\theta} \\ u_{\mathrm{s}} &= u_{\mathrm{s1}} + u_{\mathrm{s2}}, \quad u_{\mathrm{s1}} = -k_2 p. \end{aligned} \tag{10}$$

Where $u_{\mathrm{a}}$ is an adjustable model compensation control input needed for achieving perfect tracking, and $u_{\mathrm{s}}$ is a robust control law consisting of two parts: $u_{\mathrm{s1}}$ is used to stabilize the nominal system which is a proportional feedback in this case, and $u_{\mathrm{s2}}$ is a robust feedback term to attenuate the effect of model uncertainties, which will be synthesized later. Substituting (10) in to (9) and simplifying, one can obtain

$$J\dot{p} = u_{\mathrm{s}} - \varphi^{\mathrm{T}}\tilde{\theta} + \tilde{d}. \tag{11}$$

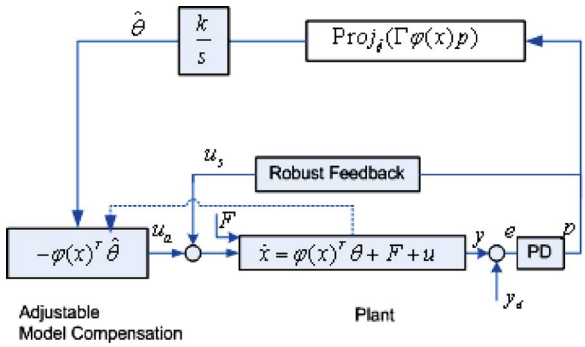


Fig. 3. ARC block diagram.

Noting Assumption 1 and P1 of (8), there exists a $u_{\mathrm{s2}}$ such that the following two conditions are satisfied:

$$\begin{aligned} &1) \quad p\left\{u_{\mathrm{s2}} - \varphi^{\mathrm{T}}\tilde{\theta} + \tilde{d}\right\} \le \varepsilon \\ &2) \quad pu_{\mathrm{s2}} \le 0 \end{aligned} \tag{12}$$

where $\varepsilon$ is a design parameter that can be chosen arbitrarily small. From condition 1), $u_{\mathrm{s2}}$ is synthesized to dominate the model uncertainties coming from both parametric uncertainties $\tilde{\theta}$ and uncertain nonlinearities $\tilde{d}$, and condition 2) guarantees that $u_{\mathrm{s2}}$ is dissipative in nature so that it does not interfere with the functionality of the adaptive control part $u_{\mathrm{a}}$. If the adaptation function in (6) is chosen as $\tau = \varphi \cdot p$ then the ARC control law in (10), whose general block diagram is depicted in Fig. 3, guarantees all signals to be bounded [11]. In addition, if after finite time $t_0$, there exist only parametric uncertainties, i.e., $(\tilde{d} = 0, \forall t \ge t_0)$, then zero final tracking error is achieved, i.e., $e \to 0$ and $p \to 0$ as $t \to \infty$.

### B. IDCARC

In the ARC design presented, the regressor $\varphi$ in the model compensation $u_{\mathrm{a}}$ (10) and adaptation function $\tau = \varphi \cdot p$ depends on the actual measurement of the velocity $x_2$. Thus, the effect of measurement noise is severe. Moreover, in spite of condition 2) of (12), there still exists a certain interaction between the model compensation $u_{\mathrm{a}}$ and the robust control $u_{\mathrm{s}}$. This may complicate the controller gain tuning process in an experimental implementation. Sadegh and Horowitz [12] proposed a desired compensation adaptation law in which the regressor is only calculated by the desired trajectory information. The idea is then incorporated in the ARC design in some other works. However, as detailed in [13], DCARC alone cannot guarantee high accuracy and disturbance attenuation as an HDD controller. Here, we introduced IDCARC, in which dynamics is added to the adaptation law. In the IDCARC, the control law and the adaptation function have the same form as (10) and $\tau = \varphi \cdot p$, respectively; however, regressor $\varphi$ is substituted by the desired regressor $\varphi_{\mathrm{d}}$

$$u = u_{\mathrm{a}} + u_{\mathrm{s}}, \qquad u_{\mathrm{a}} = -\varphi_{\mathrm{d}}^{\mathrm{T}}\hat{\theta}, \qquad \tau = \varphi_{\mathrm{d}} p \tag{13}$$

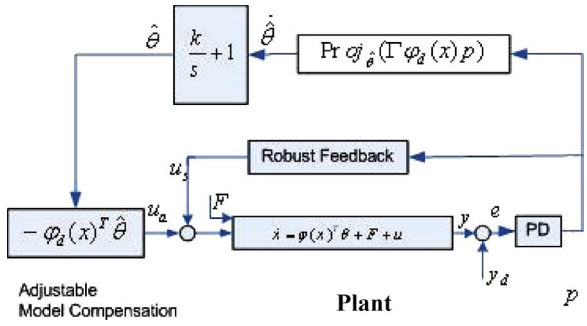


Fig. 4. IDCARC block diagram.

where $\varphi_{\mathrm{d}}^{\mathrm{T}} = [-\ddot{y}_{\mathrm{d}}, -\dot{y}_{\mathrm{d}}, -\mathrm{Sign}(\dot{y}_{\mathrm{d}}), 1]$. Substituting (13) into (11) and noting that $x_2 = \dot{y}_{\mathrm{d}} + \dot{e}$, one obtains

$$J\dot{p} = u_{\mathrm{s}} - \varphi_{\mathrm{d}}^{\mathrm{T}}\tilde{\theta} + \underline{(\theta_1 k_1 - \theta_2)\,\dot{e} + \theta_3\,[\mathrm{Sign}(\dot{y}_{\mathrm{d}}) - \mathrm{Sign}(x_2)]} + \tilde{d}. \tag{14}$$

Note that since only the desired trajectory information $y_{\mathrm{d}}(t)$ is needed in this case, the effect of noise is reduced significantly. Comparing (14) with (11), it can be seen that two additional terms (underlined) appear, which may demand a strengthened robust control function $u_{\mathrm{s}}$ for a robust performance. The strengthened robust control function $u_{\mathrm{s}}$ has the same form as (10)

$$u_{\mathrm{s}} = u_{\mathrm{s}_1} + u_{\mathrm{s}_2}, \qquad u_{\mathrm{s}_1} = -k_{\mathrm{s}_1} p. \tag{15}$$

The drawback of using the desired regressor $\varphi_{\mathrm{d}}$ instead of the measured one $\varphi$, is the inability to attenuate disturbance fast enough to accommodate HDD requirements. This is remedied in IDCARC by using a dynamical adaptation law. As depicted in Fig. 4 it is proposed to change the integrator estimator with a Proportional-Integral routine in the estimation mechanism of $\theta$. To elaborate these changes, consider the model of a hard disk servosystem in the identification procedure

$$\text{Real system}: u + d = J\ddot{y} + B\dot{y} + A_{\mathrm{f}}\mathrm{Sign}(\dot{y}_{\mathrm{d}}). \tag{16}$$

It is suggested to reach to

$$\text{Ideal system}: p = J\ddot{y}_{\mathrm{d}} + B\dot{y}_{\mathrm{d}}. \tag{17}$$

*Lemma 1:* Suppose; $y(t + t_{\mathrm{d}}) = y_{\mathrm{d}}(t)$ in which, $t_{\mathrm{d}}$ is the system time delay. Hence, for the generated signal $y(t + t_{\mathrm{d}}) \geq y(t)$, and therefore

$$y(t) = \alpha_1 y_{\mathrm{d}}(t) \text{ and } \dot{y}(t) = \alpha_2 \dot{y}_{\mathrm{d}}(t) \text{ and } \ddot{y}(t) = \alpha_3 \ddot{y}_{\mathrm{d}}(t) \tag{18}$$

where $\alpha_1$, $\alpha_2$, and $\alpha_3$ are constant coefficients depending on time. Without loss of generality, assume $u_{\mathrm{s}2} = 0$; hence, $u = u_{\mathrm{a}} + p$ by substitution of (13) into (16) with respect to (18) and some simplifications we reach

$$p + (\hat{J} - J\alpha_3)\ddot{y}_{\mathrm{d}} + (\hat{B} - B\alpha_2)\dot{y}_{\mathrm{d}} + \Big(\hat{A}_{\mathrm{f}}\mathrm{Sign}(\dot{y}_{\mathrm{d}}) - A_{\mathrm{f}}\mathrm{Sign}(\alpha_2\dot{y}_{\mathrm{d}})\Big) + (d - \hat{d}) = 0. \tag{19}$$

Now, we propose adding a dynamic term to $u_{\mathrm{a}}$

$$p + (\dot{\hat{J}}\ddot{y}_{\mathrm{d}} + k\hat{J}\dddot{y}_{\mathrm{d}} - J\alpha_3\ddot{y}_{\mathrm{d}}) + (\dot{\hat{B}}\dot{y}_{\mathrm{d}} + k\hat{B}\ddot{y}_{\mathrm{d}} - B\alpha_2\dot{y}_{\mathrm{d}}) + \Big(\dot{\hat{A}}_{\mathrm{f}}\mathrm{Sign}(\dot{y}_{\mathrm{d}}) + k\hat{A}_{\mathrm{f}}\mathrm{Sign}(\dot{y}_{\mathrm{d}}) - A_{\mathrm{f}}\mathrm{Sign}(\alpha_2\dot{y}_{\mathrm{d}})\Big) + (d - \dot{\hat{d}} - k\hat{d}) = 0. \tag{20}$$

Furthermore, each term inside the brackets consists of a first-order differential equation, i.e., by this means a suitable dynamics is introduced for the compensation signal. Since, by the introduced dynamics, (16) approaches to (17) dynamically, hence better disturbance and friction compensation are obtained. Thus, the adaptation law can be interpreted as adding an integrator proportional to $u_{\mathrm{a}}$, as depicted in Fig. 4. The proposed improved IDCARC law and the adaptation function have the same form as (13), respectively, but with the difference that $\tau = \varphi_{\mathrm{d}} \cdot p$ is subjected to the introduced dynamics of $\tau_{\mathrm{d}}$ as

$$u = u_{\mathrm{a}} + u_{\mathrm{s}}, \quad u_{\mathrm{a}} = -\varphi_{\mathrm{d}}^{\mathrm{T}}\hat{\theta}, \quad \tau_{\mathrm{d}} = \varphi_{\mathrm{d}}(\dot{p} + kp). \tag{21}$$

Equations (13)–(18) can be applied with this improvement to IDCARC. One can write (14) as

$$\dot{p} = u_{\mathrm{s}} - \varphi_{\mathrm{d}}^{\mathrm{T}}(\tilde{\theta}) + (\theta_1 k_1 - \theta_2)\dot{e} + \theta_3\,[\mathrm{Sign}(\dot{y}_{\mathrm{d}}) - \mathrm{Sign}(x_2)] + \tilde{d} \tag{22}$$

where $\tilde{\theta} = (\hat{\theta} + k\dot{\hat{\theta}}) - \theta$. Applying mean value theorem, we have

$$\mathrm{Sign}(x_2) - \mathrm{Sign}(\dot{y}_{\mathrm{d}}) = g(x_2, t)\dot{e}, \tag{23}$$

in which $g(x_2, t)$ is a nonlinear function. The strengthened robust control function $u_{\mathrm{s}}$ has the same form as (10)

$$u_{\mathrm{s}} = u_{\mathrm{s}1} + u_{\mathrm{s}2}, \qquad u_{\mathrm{s}1} = -k_{\mathrm{s}1} p \tag{24}$$

but with $k_{\mathrm{s}1}$ being a nonlinear function. We must have $k_{\mathrm{s}1} \geq k_2 + \theta_1 k_1 - \theta_2 - \theta_3 g + (\theta_2 + \theta_3 g)^2 / 2\theta_1 k_1$ such that the matrix A defined below becomes positive definite

$$A = \begin{bmatrix} k_{\mathrm{s}1} - k_2 - \theta_1 k_1 + \theta_2 + \theta_3 g & -\frac{1}{2}k_1(\theta_2 + \theta_3 g) \\ -\frac{1}{2}k_1(\theta_2 + \theta_3 g) & \frac{1}{2}Jk_1^3 \end{bmatrix} \tag{25}$$

$u_{\mathrm{s}2}$ is required to satisfy following constraints similar to (12):

$$\begin{aligned} &1) \quad p\left\{u_{\mathrm{s}2} - \varphi_{\mathrm{d}}^{\mathrm{T}}\tilde{\theta} + \tilde{d}\right\} \leq \varepsilon \\ &2) \quad pu_{\mathrm{s}2} \leq 0. \end{aligned} \tag{26}$$

As shown in Fig. 5, because of the additional term in (22), the robust term of IDCARC $u_{\mathrm{s}}$ in (24) must be stronger than the robust term of ARC, whereas the better adaptation mechanism in IDCARC causes lower upper bounds for $p^2(t)$ in IDCARC; simulations confirm this general observation.

*Theorem 1:* If the IDCARC law (14) is applied, then

1) In general, all signals are bounded. Furthermore, the positive definite function

$$V_{\mathrm{s}} = 1/2Jp^2 + 1/2Jk_1^2e^2. \tag{27}$$

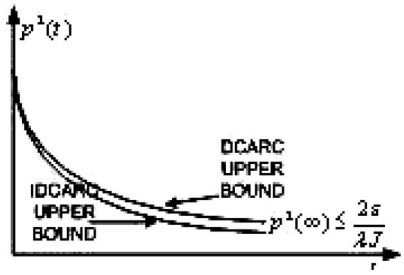


Fig. 5. Upper bound of $p^2(t)$ in ARC and IDCARC.

is bounded by

$$V_{\rm s} \le \exp(-\lambda t)V_{\rm s}(0) + \frac{\varepsilon}{\lambda}\left[1 - \exp(-\lambda t)\right] \tag{28}$$

where $\lambda = \min\{2k_2/\theta_{1\max}, k_1\}$.

2) If after finite time $t_0$, there exist parametric uncertainties only (i.e., $\tilde{d} = 0, \forall t \ge t$) then, in addition to the result in 1), zero final tracking error is also achieved, i.e.: $e \to 0$ and $p \to 0$ as $t \to \infty$.

*Proof:* Along the trajectory of (20), the time derivative of $V_{\rm s}$ given by (27) is

$$\dot{V}_{\rm s} = p\left\{u_{\rm s} - \varphi_{\rm d}^{\rm T}\tilde{\theta} + (\theta_1 k_1 - \theta_2)\dot{e} + \theta_3 \times \left[S_{\rm f}(\dot{y}_{\rm d}) - S_{\rm f}(x_2)\right] + \tilde{d}\right\} + Jk_1^2 e\dot{e}. \tag{29}$$

Applying (23) and (24) whereas $\dot{e} = p - k_1 e$ and $\theta_1 = J$, we have

$$\dot{V}_{\rm s} \le p\left\{u_{\rm s2} - \varphi_{\rm d}^{\rm T}\tilde{\theta} + \tilde{d}\right\} + \left(-k_{\rm s1} + \theta_1 k_1 - \theta_2 - \theta_3 g\right)p^2 + k_1\left(\theta_2 + \theta_3 g\right)ep - Jk_1^3 e^2. \tag{30}$$

If $A$ given by (25) is positive definite, then

$$\dot{V}_{\rm s} \le p\left\{u_{\rm s2} - \varphi_{\rm d}^{\rm T}\tilde{\theta} + \tilde{d}\right\} + k_2 p^2 - \frac{1}{2}Jk_1^3 e^2. \tag{31}$$

With condition 1) of (26) and $\lambda = \min\{2k_2/\theta_{1\max}, k_1\}$, the derivative of $V_{\rm s}$ becomes

$$\dot{V}_{\rm s} \le -\lambda V_{\rm s} + \varepsilon. \tag{32}$$

Which leads to (28) and the results in 1) are proved. Now, consider a situation on 2) where $\tilde{d} = 0$, $\forall t \ge t_0$. Choose a positive definite function $V_{\rm a}$ as

$$V_{\rm a} = V_{\rm s} + \frac{1}{2}\tilde{\theta}^{\rm T}\Gamma^{-1}\tilde{\theta}. \tag{33}$$

From (30), condition 2) of (26), and P2 of (8), the derivative of $V_{\rm a}$ satisfies

$$\dot{V}_{\rm a} \le -k_2 p^2 - \frac{1}{2}Jk_1^3 e^2 + \tilde{\theta}^{\rm T}\Gamma^{-1}(\dot{\hat{\theta}} - \Gamma\tau) \le W \tag{34}$$

where $W = -k_2 p^2 - (1/2)Jk_1^3 e^2$. Therefore, $W \in L_1$ and $V_{\rm a} \in L_\infty$. Since all signals are bounded, and it is easy to check $\dot{W}$ is bounded and thus uniformly continuous. By Barbalet's lemma $W \to 0$ as $t \to 0$. ■

*Remark:* Let $h$ be any smooth function satisfying: $h \ge \|\theta_{\rm M}\|\ \|\varphi\| + \delta_{\rm d}$ where $\theta_{\rm M} = \theta_{\max} - \theta_{\min}$. Then, one smooth example of $u_{\rm s2}$ satisfying (12) is given by: $u_{\rm s2} = -(1/4\varepsilon)h'^2 p$, also for (26): $h' \ge \|\theta_{\rm M}\|\ \|\varphi_{\rm d}\| + \delta_{\rm d}$, $u_{\rm s2} = -(1/4\varepsilon)h'^2 p$.

## IV. Comparative Studies

### A. Performance Indices

Simulation studies have been performed for ARC, DCARC, and IDCARC to verify the effectiveness of the proposed controller in terms of tracking errors and disturbance rejection. To compare the simulation results for representatives of different controllers proposed for such systems as in the literature [4], [6], [7], the following performance indices are used.

1) $L_2[e] = \sqrt{(1/T_{\rm f})\int_0^{T_{\rm f}} |e|^2 dt}$ is an average tracking performance index, for the entire error curve $e(t)$. $T_{\rm f}$ represents the total simulation time.
2) $e_{\rm M} = \max_t\{|e(t)|\}$, is the maximum absolute value of the tracking error.
3) $e_{\rm f} = \max_{T_{f-1} \le t \le T_{\rm f}}\{|e(t)|\}$, is the maximum absolute value of the tracking error during the last millisecond.
4) $L_2[u] = \sqrt{(1/T_{\rm f})\int_0^{T_{\rm f}} |u|^2 dt}$, is the mean of the control input.
5) $c_u = L_2[\Delta u]/L_2[u]$, is the control input chattering, where : $L_2[\Delta u] = \sqrt{(1/N)\sum_{j=1}^{N} |u(j\Delta T) - u((j-1)\Delta T)|^2}$ is the normalized control variations.

### B. Controller Structures

The following control structures are used in simulations.

1) **MSC:** During the seeking mode of MSC, the servo-controller drives the read/write head to follow the desired velocity profile, which is calculated base on a rigid body plant model. Defining the velocity profile as $\nu(p) = -\mathrm{sgn}(p)\sqrt{2a|p|} - r_t$ if $|p| > 2r_t^2/a$ or $\nu(p) = -(a/2r_t)$. $p$ if $|p| < 2r_t^2/a$ a PTOS can be generated [1]. In which, $p$, $a$, and $r_t$ are the remaining distance to the target track, the maximum acceleration, and the velocity offset, respectively. In the PTOS approach, the back electromotive force, which physically behaves like a linear friction, and the actuator bandwidth, are not taken into consideration and as a result, the velocity profile in PTOS method can only be approximately followed.
2) **ARC:** The ARC law proposed in Section III is applied on the system. With $u_{\rm s} = -k_{\rm s}p$, $k_{\rm s} \ge k_2 + h^2/4\varepsilon$ the control gains are chosen as: $k_1 = 317$ to have a bandwidth of about 500 Hz, and $k_{\rm s} = 1.0$. The adaptation rates are set as $\Gamma = \mathrm{diag}\{10, 0, 1, 10\,000\}$. The initial parameters are chosen as follows:

$$\hat{\theta}(0) = [1e-6, 12.5e-6, 0, 0]^{\rm T}$$

$$\theta_{\max} = [0.8e-6, 1e-5, 0.5]^{\rm T}.$$

3) **DCARC:** The DCARC law with $u_{\rm s} = -k'_{\rm s}p$ is applied on the system. The control gains are chosen as

TABLE II
PERFORMANCE INDEX FOR DESIRED TRAJECTORY

| Experiments | Set 1 | | | Set 2 | | | Set 3 | | |
|---|---|---|---|---|---|---|---|---|---|
| Performance Index | ARC | DCARC | IDCARC | ARC | DCARC | IDCARC | ARC | DCARC | IDCARC |
| $e_M \times 10^{-4}$ | 1.48 | 1.82 | 7.47e-4 | 1.82 | 1.48 | 7.47e-4 | 1.76 | 2.78 | 9.34e-4 |
| $e_F \times 10^{-6}$ | 0.26 | 1.21 | 2.04e-4 | 8.9 | 8.45 | 5.25e-3 | 7.83 | 2.2e1 | 5.19e-3 |
| $L_2[e] \times 10^{-4}$ | 6.5 | 7.48 | 3.2e-3 | 8.11 | 6.71 | 3.83e-3 | 7.78 | 13 | 4.51e-3 |
| $L_2[u] \times 10^{-2}$ | 0.49 | 0.66 | 0.44 | 0.68 | 0.50 | 0.45 | 0.64 | 1.10 | 0.56 |
| $L_2[\Delta u] \times 10^{-4}$ | 1.05 | 0.75 | 0.77 | 0.84 | 1.10 | 0.93 | 1.39 | 1.36 | 1.09 |
| $c_u \times 10^{-2}$ | 2.15 | 1.14 | 1.74 | 1.25 | 2.2 | 2.08 | 2.17 | 1.24 | 1.98 |

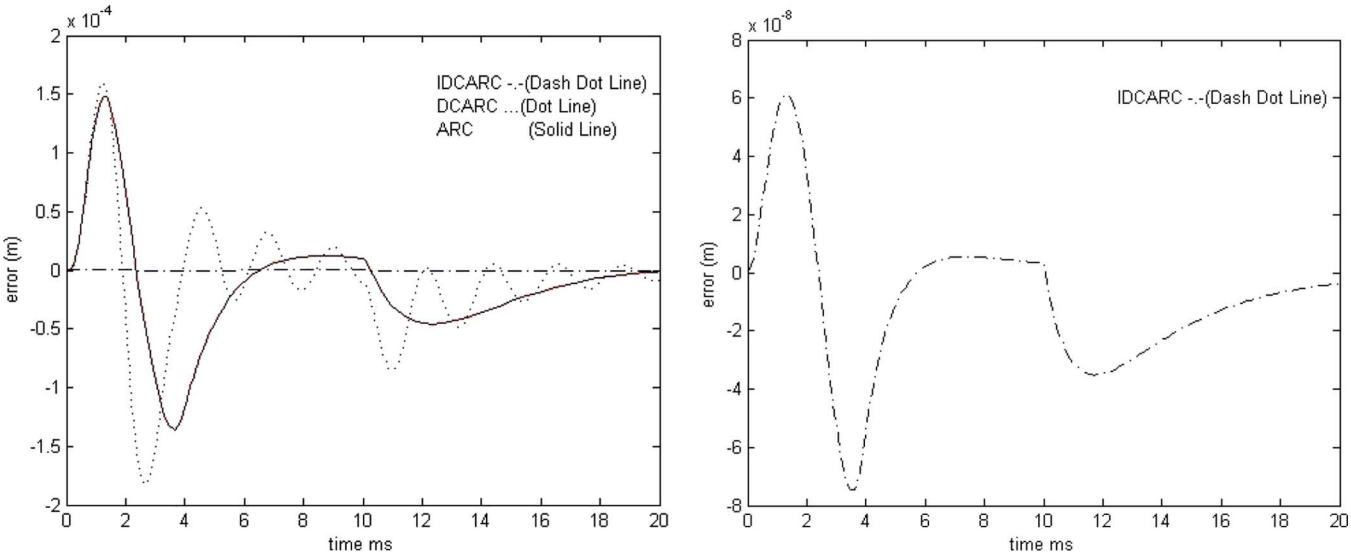


Fig. 6. Tracking error for different methods.

$k_s' \geq k_2 + h'^2/4\varepsilon$ to have a bandwidth of about 500 Hz $k_1 = 317$ and $k_s' = 1.0$. The adaptation rates are set as $\Gamma = \text{diag}\{10, 0, 1, 10\,000\}$.

4) **IDCARC:** The proposed IDCARC law is applied on the system. All coefficients are the same as DCARC coefficient and integrator gain in adaptive part is set to $k = 1000$.

### C. Simulation Input Signals

To have a fair comparison, the following sets of simulation input signals are considered.

- Set 1: To test tracking performance of the controllers in the presence of friction with $A_f = 1e-5$ as in [3], a 2600 track seeking trajectory is considered in this set, as elaborated in [13] and illustrated in Fig. 10.
- Set 2: A step disturbance input at $t = 10$ ms with amplitude of about 0.5 mA is considered in this set in addition to the above reference trajectory.
- Set 3: The performance of the Set 1) reference trajectory in the presence of 20% variation in system gain is simulated in this set.

### D. Controller Performance

As quantitatively shown in Table II, the simulation result in terms of performance indices $e_M$ and $e_f$ of IDCARC is significantly better than that of ARC and DCARC for all sets, specifically in the presence of disturbance. As shown in Figs. 6 and 7 it has been observed that ARC is relatively poor in rejecting disturbance compared to the IDCARC. IDCARC has the best performance in terms of $L_2[u]$, $L_2[e]$, $e_M$, and $e_f$ for all aforementioned sets. The main reason for this significant improvement is due to the proposed dynamic term added in the estimation procedure. It can be seen in Fig. 6 that the closed loop position results obtained through the IDCARC method, have suitable settling characteristics without any large overshoot and attenuate disturbances extremely better than ARC. It is observed that for larger disturbances ARC becomes unstable but IDCARC can still attenuate disturbances relatively well. To analyze the other important issues on the performance of the closed loop system, the control efforts are illustrated in Fig. 7. As shown in this figure, the smooth control effort confirms the advantages of jerk-minimized reference input, especially at the time of disturbance enforcement at $t = 10$ ms. Moreover, the low values of obtained errors in the IDCARC method shows the effectiveness of delay compensation. The rejection

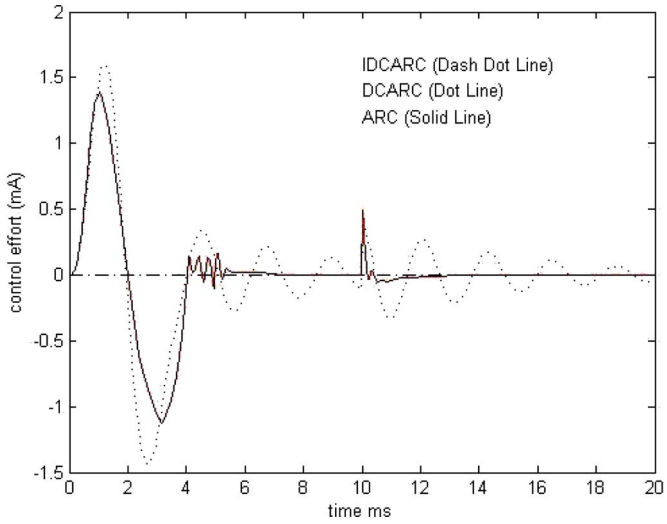


Fig. 7. Control effort for smooth signal generated.

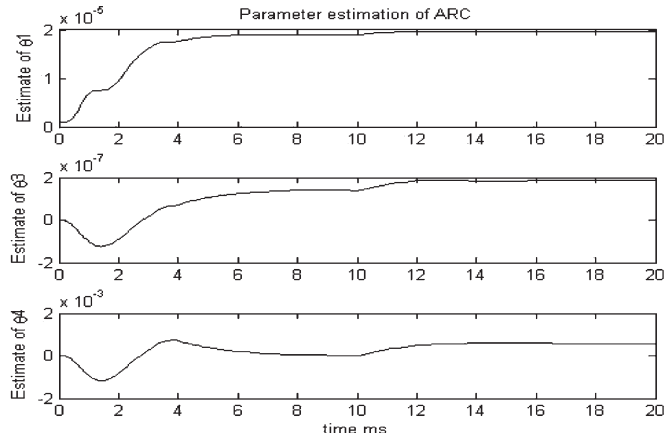


Fig. 8. Parameter estimation of ARC.

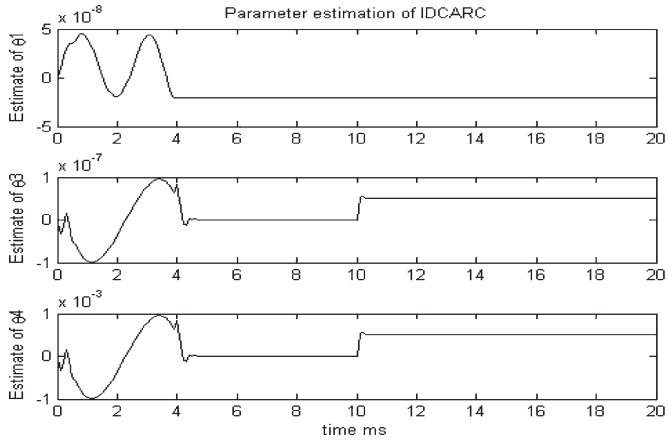


Fig. 9. Parameter estimation of IDCARC.

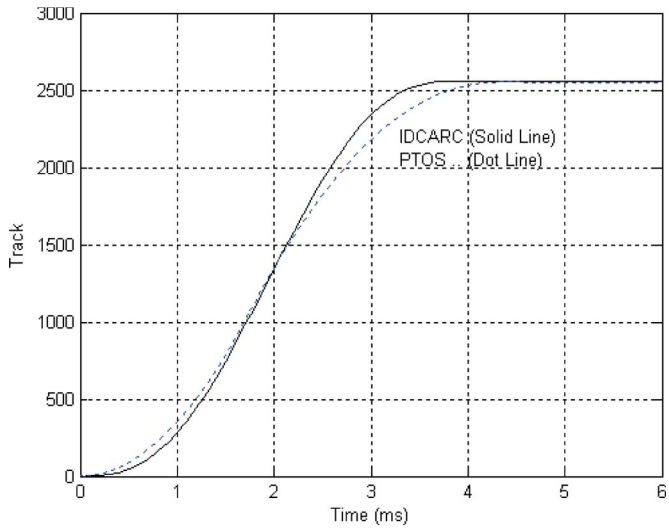


Fig. 10. Seeking and following of 2600 tracks.

of the disturbance occurring at $t = 10$ ms in the IDCARC method shows superior characteristics in the presence of higher frequency modes considered in the simulated model. Because of the introduced dynamics in adaptation algorithm in the IDCARC method, the proposed method is capable of picking up the actual value of disturbance more quickly. This can be seen from the comparison of the parameter estimation rates shown in Figs. 8 and 9, in which in the IDCARC method, the steady state convergence of the parameters are much faster than that in ARC. Finally, as illustrated in Fig. 10 the track seeking time of IDCARC results are much faster than that in the conventional PTOS method.

### *E. Runout Disturbance and Position Error Signal (PES)*

The disturbances in a real HDD are usually considered as a lumped disturbance at the plant outputs, known as runouts, [16]. Repeatable runouts are caused by spindle motor rotation, and consist of frequencies that are multiple spindle frequencies. Nonrepeatable runouts, on the other hand, are caused mainly due to vibrations and shocks, mechanical disturbance and electrical noise, and hence, usually random and unpredictable. Although the effects of the runouts are not considered in our problem formulation, it turns out that the proposed controller is capable of rejecting the few first modes of the runout disturbances quite effectively. Fig. 11 shows the tracking error of ARC and IDCARC controllers, under the simulated disturbance of runouts as in [16]. It is illustrated in this figure how effective is the proposed IDCARC method in runout rejection compared to that of the ARC method. To get comprehensive performance verification in the presence of runout disturbance, the statistical measure of PES can be analyzed. In disk drive applications, the variation of the R/W head from the center of track during track following, which can be directly read off as the PES, is very important. The HDD servosystem must ensure that PES is kept to a minimum. Having deviations that are above the tolerance of the disk drive would result in too many R/W errors, making the disk drive unusable. A suitable measure is the standard deviation of the readings, $\sigma_{\rm pes}$. A useful guideline is to make the $3\sigma_{\rm pes}$ value $< 10\%$ of the track pitch, which is about 0.1 $\mu$m for a track density of 25 kTPI. In the simulations made for the system in hand, the $3\sigma_{\rm pes}$ value for the ARC controller is about 0.0335 $\mu$m and for the IDCARC is 1.4238e-5 $\mu$m, which shows a significant improvement in terms of disturbance rejection. In case of DCARC the $3\sigma_{\rm pes}$ value is more than 0.1 $\mu$m and not acceptable. By this comparison study, the effectiveness of

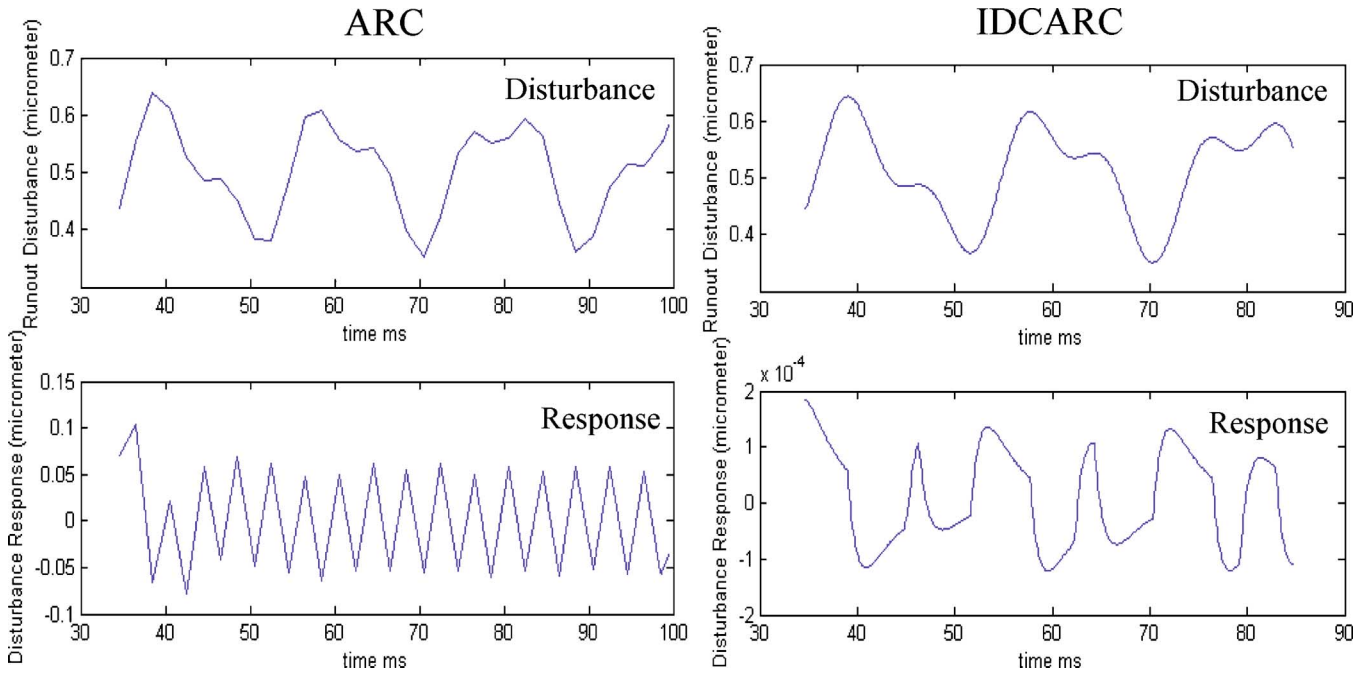


Fig. 11. Runout disturbance and response in ARC and IDCARC methods.

the proposed control algorithm is verified and compared to the other methods.

## V. Conclusion

In this paper, an ARC is implemented for HDDs, considering high frequency modes in the model. This method with its unified structure can be applied to both seeking and following modes.

In this proposed method a discontinuous projection based on the ARC is considered first. This controller theoretically guarantees a prescribed transient performance and well behaved tracking in the presence of parametric uncertainties. An IDCARC scheme is then proposed, in which the adaptation regressor is calculated using only reference trajectory information. The resulting controller has many implementation advantages. It reduces not only the on-line computation time, but also the induced structural vibration, the effect of the measurement noise, and moreover, it separates the robust control design from parameter adaptation with a faster adaptation rate. A thorough robust analysis of this method is presented first, in which a controller designed based on a simple model of the system is implemented in closed loop on a more comprehensive model for the system. The simulation result verifies the robustness and the significant performance improvement of the IDCARC compared to that of ARC for this model. Moreover, the simulation and comparison results illustrate the ability of the proposed method in achieving suitable control in the presence of unstructured model uncertainties, and input disturbances. It is shown that the IDCARC method is capable of significantly improving the seeking and following performances, and its implementation on a more comprehensive model of the system provides the assurance of its successful experimental implementation.

## References

[1] B. Hredzak, G. Hermann, and G. Guo, "A proximate-time-optimal-control design and its application to a hard disk drive dual-stage actuator system," *IEEE Trans. Magn.*, vol. 42, no. 6, pp. 1708–1715, Jun. 2006.

[2] Y. Li, V. Venkataramanan, G. Guo, and Y. Wang, "Dynamic nonlinear control for fast seek-settling performance in hard disk drives," *IEEE Trans. Ind. Electron.*, vol. 54, no. 2, pp. 951–962, Apr. 2007.

[3] L. Yi and M. Tomizuka, "Two-degree-of-freedom control with adaptive robust control for hard disk servo systems," *IEEE/ASME Trans. Mechatronics*, vol. 4, no. 1, pp. 17–24, Mar. 1999.

[4] S. Hara, T. Hara, L. Yi, and M. Tomizuka, "Novel reference signal generation for two degree-of-freedom controllers for hard disk drives," *IEEE/ASME Trans. Mechatronics*, vol. 5, no. 1, pp. 73–78, Mar. 2000.

[5] J. Ishikawa, Y. Yanagita, T. Hattori, and M. Hashimoto, "Head positioning control for low sampling rate systems based on two degree-of-freedom control," *IEEE Trans. Magn.*, vol. 32, no. 2, pp. 1787–1792, May 1996.

[6] C. K. Pang, F. L. Lewis, S. S. Ge, G. Guo, B. M. Chen, and T. H. Lee, "Singular perturbation control for vibration rejection in HDDs using the PZT active suspension as fast subsystem observer," *IEEE Trans. Ind. Electron.*, vol. 54, no. 3, pp. 1375–1386, Jun. 2007.

[7] B. M. Chen, T. H. Lee, and V. Venkataramanan, "Composite nonlinear feedback control for linear systems with input saturation: Theory and application," *IEEE Trans. Autom. Control*, vol. 48, no. 3, pp. 427–439, Mar. 2003.

[8] Q. Hao, R. Chen, G. Guo, S. Chen, and T. S. Low, "A gradient-based track-following controller optimization for hard disk drive," *IEEE Trans. Ind. Electron.*, vol. 50, no. 1, pp. 108–115, Feb. 2003.

[9] K. Peng, B. M. Chen, G. Cheng, and T. H. Lee, "Modeling and compensation of nonlinearities and friction in a micro hard disk drive servo system with nonlinear feedback control," *IEEE Trans. Control Syst. Technol.*, vol. 13, no. 5, pp. 708–721, Sep. 2005.

[10] C. Du, L. Xie, J. N. Teoh, and G. Guo, "An improved mixed $H_2/H_\infty$ control design for hard disk drives," *IEEE Trans. Control Syst. Technol.*, vol. 13, no. 5, pp. 832–839, Sep. 2005.

[11] L. Xu and B. Yao, "Adaptive robust precision motion control of linear motors with negligible electrical dynamics: Theory and experiments," *IEEE/ASME Trans. Mechatronics*, vol. 6, no. 4, pp. 444–452, Dec. 2001.

[12] N. Sadegh and R. Horowitz, "Stability and robustness analysis of a class of adaptive controllers for robot manipulators," *Int. J. Robot. Res.*, vol. 9, no. 3, pp. 74–92, Jun. 1990.

[13] E. Jamei and H. D. Taghirad, "Adaptive robust controller synthesis for hard disk servo systems," in *Proc. IEEE/RJS, Conf. Intel. Robots Syst.*, Sendai, Japan, 2004, pp. 1154–1159.

[14] B. Yao, "High performance adaptive robust control of nonlinear systems: A general framework and new schemes," in *Proc. IEEE Conf. Decision Control*, San Diego, CA, 1997, pp. 2489–2494.

[15] B. Yao and M. Tomizuka, "Smooth robust adaptive sliding mode control of robot manipulators with guaranteed transient performance," *Trans. ASME, J. Dyn. Syst. Meas. Control*, vol. 118, no. 4, pp. 764–775, 1996.
[16] V. Venkataramanan, B. M. Chen, T. H. Lee, and G. Guo, "A new approach to the design of mode switching control in hard disk drive servo systems," *Control Eng. Pract.*, vol. 10, no. 9, pp. 925–939, Sep. 2002.

**Hamid D. Taghirad** (S'96–M'97) received the B.Sc. degree in mechanical engineering from Sharif University of Technology, Tehran, Iran, in 1989 and the M.Eng. degree in mechanical engineering and the Ph.D. degree in electrical engineering from McGill University, Montreal, Canada, in 1993 and 1997, respectively.

He is currently an Associate Professor with the Department of Electrical Engineering and the Director of the Office of International and Scientific Cooperation, K. N. Toosi University of Technology, Tehran. He is also a Cofounder of the Advanced Robotics and Automated System (ARAS) Research Group. He is the author of two books and more than 90 papers in international journals and conference proceedings. His research interests include robust and nonlinear control applied on robotic systems.

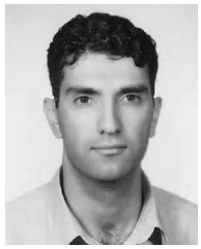

**Ehsan Jamei** received the B.Sc. degree in electrical engineering from Sahand University of Technology, Tabriz, Iran, in 2000 and the M.Eng. degree in electrical engineering from K. N. Toosi University of Technology, Tehran, Iran, in 2003.

He is currently with the Advanced Robotics and Automated Systems (ARAS) Research Group, Department of Electrical Engineering, K. N. Toosi University of Technology. His research interests include industrial automation and the design and control of mechatronics systems.